POLITECNICO DI TORINO
Repository ISTITUZIONALE

Aerial urban observation to enhance energy assessment and planning towards climate-neutrality: A pilot application to the city of Turin

Original
Aerial urban observation to enhance energy assessment and planning towards climate-neutrality: A pilot application to the city of Turin / Anselmo, S., Ferrara, M., Corgnati, S.P., Boccardo, P.. - In: SUSTAINABLE CITIES AND SOCIETY. - ISSN 2210-6707. - ELETTRONICO. - 99:(2023), p. 104938. [10.1016/j.scs.2023.104938]

Availability:
This version is available at: 11583/2983566 since: 2023-11-03T09:10:44Z

Publisher:
Elsevier

Published
DOI:10.1016/j.scs.2023.104938

Terms of use:

This article is made available under terms and conditions as specified in the corresponding bibliographic description in the repository

Publisher copyright

(Article begins on next page)

26 November 2026

Sustainable Cities and Society 99 (2023) 104938



Contents lists available at ScienceDirect

Sustainable Cities and Society

journal homepage: www.elsevier.com/locate/scs

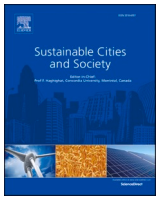



Aerial urban observation to enhance energy assessment and planning towards climate-neutrality: A pilot application to the city of Turin

Sebastiano Anselmo [a], Maria Ferrara [b,*], Stefano Paolo Corgnati [b], Piero Boccardo [a]

[a] Interuniversity Department of Regional and Urban Studies and Planning, Politecnico di Torino, Italy
[b] Department of Energy, Politecnico di Torino, Italy

ARTICLE INFO

Keywords:
Remote sensing
Earth observation
Infrared thermography
Energy planning
Data mining for urban building energy modelling
science-based decision making

ABSTRACT

Based on the central role of cities in the decarbonisation process, this study aims at providing a novel methodology to assess and optimize the building energy demand and photovoltaic producibility at city scale. This is done by exploring the potential of aerial acquisition of local-scale thermographic data to integrate the existing database on building Energy Performance Certificates, on which the EU energy assessment and retrofit policies are based, on a dedicated GIS platform. Once the method is validated through testing the reliability of the resulting energy classification of buildings, the approach is used to esteem the energy demand and potential energy production in the current state and two alternative retrofit scenarios for a large district in Turin, Italy. For the analysed scenarios, potential savings are quantified up to 20 GWh and 5000 tCO_2 yearly, decreasing by more than 70 % primary energy and CO_2 emissions when photovoltaic panels and heat pumps are optimally used and integrated to the existing district heating system. Conclusions remark the potential of this tool to support urban policy making and governance, also with the future perspective of a thematic urban digital twin for planning energy retrofit intervention and large scale implementation of Renewable Energy Communities.

1. Introduction

In the current context of energy transition, the building sector is playing a major role in accelerating urban transformation towards decarbonisation objectives.

As urban population continues to grow, energy demand and emissions concentrate in urban areas and the current European climate policies recognize the urgent need to implement strategies enabling cities' sustainable development and encouraging a transition towards post-carbon cities. The recent fit for 55 package aims to bring EU legislation in line with the 2030 EU's target of reducing net greenhouse gas emissions by at least 55 % (European Commission 2021), towards the objective of the European Commission Roadmap aiming for an 80-95 % reduction of EU GHG emissions by 2050 (compared with 1990 levels) (European Commission 2011). The European call for 100 climate neutral cities by 2030, defined as one of the Mission to tackle major challenges in the framework of Horizon Europe (Commission announces 100 cities participating in EU, 2021), was born in this context and highlights the crucial role of cities in driving decarbonization, in line with the United Nations 2030 Agenda for Sustainable Development (UN, 2015), where the SDG 11 –"Make cities and human settlements inclusive, safe, resilient and sustainable"- identifies the city as a key area of intervention in the path towards a post-carbon society to deal with mitigation and adaptation to climate change.

This renewed the academic and institutional debate around the urgent need for providing easy and effective methodologies to support local government and institutions in integrating available data and tools to support the urban energy planning and strategies for decarbonisation (Shang & Lv, 2023). The recent research advancements have largely addressed the technological barriers for optimizing the energy performance of buildings (advanced materials and components to increase the building envelope efficiency and reduce energy demand, efficient energy systems exploiting energy from renewable sources), as envisioned by latest report on energy technology perspectives by International Energy Agency (IEA, 2020). Therefore, reaching the targeted levels of decarbonization is now a matter of policy makers and governance bodies, who will have to decide for retrofit strategies in a complex set of different local economic, social and spatial constraints.

In particular, the new European directive on the energy performance of buildings EPBD approved in March 2023 (P9_TA 2021) poses two major challenges for the existing building stock: 1) the phasing out of fossil fuels in buildings and the consequent trend to electrification; 2) the achievement of minimum performance objectives for all existing

* Corresponding author.
E-mail address: maria.ferrara@polito.it (M. Ferrara).

https://doi.org/10.1016/j.scs.2023.104938
Received 13 April 2023; Received in revised form 13 September 2023; Accepted 14 September 2023
Available online 15 September 2023
2210-6707/© 2023 The Author(s). Published by Elsevier Ltd. This is an open access article under the CC BY license (http://creativecommons.org/licenses/by/4.0/).

Nomenclature

AUC	Area Under the Curve
CO_2	Carbon Dioxide
DH	District Heating
DHW	Domestic Hot Water
DSM	Digital Surface Model
EED	Energy Efficiency Directive
EPBD	Energy Performance of Buildings Directive
EPC	Energy Performance Certificate
EU	European Union
G	Gas
GEPI	Global Energy Performance Index
GHG	Green House Gas
GIS	Geographic Information System
HD	High Definition
HP	Heat Pump
ISTAT	*Istituto Nazionale di Statistica* (Italian Statistical Institute)
LiDAR	Light Detection And Ranging
MWIR	Midwave Infrared
MP	Mega Pixel
PI	Performance Index
PV	PhotoVoltaic
RED	Renewable Energy Directive
ROC	Receiver Operating Curve
SDG	Sustainable Development Goal
UAV	Unmanned Aerial Vehicle

buildings measured in terms of improvement of energy performance class of the building, which can derive from a combination of actions aimed to reduce the building energy demand and increase their coverage from renewable energy sources. Since the introduction in the first EPBD of 2002 (Directive 2002/91/EC, 2022) many buildings and building units have been classified with an Energy Performance Certificate (EPC) as required before any intervention (sell/acquisitions, within a renovation process...). Recognizing the potential of this dataset on the energy performance of existing buildings (Pasichnyi et al., 2019), the new revised EPBD has just reinforced the role of EPC in driving policies to increase the energy performance of buildings, defining targets in terms of energy class improvement.

Pursuing these objectives requires identifying the worst-performing buildings on which it is essential to prioritize energy retrofit interventions for the required energy class upgrade. Therefore, mapping the status of the building stock and classifying the energy performance of the different buildings is essential, but the existing set of EPCs does not cover the entire building stock and, because the EPC is required in case of retrofit interventions, it often happens that buildings that do not have a current EPC are also buildings with low energy performance.

In the current context, this dataset should be integrated with other data sources or calculation models that provide information on the energy performance of the buildings in a defined urban area, finding an appropriate trade-off between data accuracy and manageability.

1.1. Background

Regarding the assessment of building energy consumptions at city levels, urban-scale building energy modeling (UBEM) techniques can be used. However, detailed bottom-up physics-based approach (Ferrando et al., 2020) may be too expensive to be used to gather data about the current status of the building stock and plan for retrofit interventions, mainly due to the fact that detailed data on a building-by-building basis may be difficult to obtain (Deng et al., 2023) – in fact, such approaches often rely on the use of building archetypes. Further, the accuracy of UBEMs is often questionable and depends on the level of data aggregation, with errors ranging from 1-19 % at annual aggregate resolutions (Fonseca & Schlueter, 2015) to 1000 % for single buildings (Oraiopoulos & Howard, 2022).

In their recent study, Johari et al. (2023) explore the use of EPC data to develop and calibrate georeferenced UBEMs for two cities in Sweden. Results are promising and show that EPC data may constitute a valid data source for UBEM at city scale, with registered errors ranging between 26 % for single buildings to 10 % at city level. Also, their study highlights how georeferencing is crucial to support the correct understanding of existing dataset. Geographic Information Systems (GIS) are recognized as powerful tools to integrate multiple data layers with spatial resolution for UBEMs (Yu et al., 2021) and, if the temporal dimension is also addressed by appropriate data evolution over time, GIS-informed urban energy modeling may be seen as digital-twins for energy planning and management at city scale (Xia et al., 2022). However, the current archetype-based approach highlights the need for other data sources to be able to extend the analysis to all buildings for which georeferenced EPCs and other data are missing.

In their recent review on data acquisition for UBEMs, Wang et al. (2022) show how aerial data acquisition is recognized as a valid data source for georeferenced UBEMs, especially for geometrical data acquired by means of the LiDAR technique. However, no reference is provided about the use of thermography. A recent review by Martin et al. (2022) highlights that many studies have investigated the great potential of thermographic analysis in applications to the built environment. Different scales relate to different acquisition techniques: thermal-related problems may be addressed at the microscale, by simply using a thermal camera on a handheld systems or, at the district or city scale, with the support of infrared cameras installed on aerial vehicles such as drones (unmanned aerial vehicles, for neighborhood to district studies) or aircrafts or helicopters (for studies at district or city levels), up to a territorial scale where sensors are placed on satellites for collection of remotely sensed data. The literature review shows that most studies using thermography are conducted at single-building scale, for detecting degradation of building envelope or systems faults (Zheng et al., 2022), for energy audit or, in the field of whole building energy performance assessment, for building energy model calibration (Bayomi et al., 2021). Instead, when thermography is approached at district of city scale, studies focus on observing the urban heat island effect or analyzing city heat fluxes, including urban infrastructures such as district energy systems (Zhou et al., 2018). So far, the use of aerial thermography for the urban energy modelling has been investigated by Bitelli et al. (2015) for the city of Bologna, Italy. Recognizing the difficulties in calibrating the acquired data for developing accurate physics-based building energy models, they highlight the extremely high need of integration with additional data (e.g., geometric data or existing EPCs). Thus, it appears that the use of aerial thermography for building energy performance assessment and classification is still unexplored.

1.2. Scope, novelty and structure of the work

Recognizing urban remote sensing, and aerial survey in particular, as a quick and efficient way to collect time-synchronized building-related data at district and city scale (Yu & Fang, 2023), and that aerial infrared thermography is essentially a form of geospatial data, its untapped potential emerges from literature review, which exposes a notable lack of recognition of such data in the geospatial realm and its integration in GIS, towards new energy-related applications in the built environment in the current context of new regulatory requirements imposed by the ongoing energy transition.

This study aims at integrating and mining geometric and thermographic data acquired from aerial surveys to the existing database on building Energy Performance Certificates on a dedicated GIS platform to be used for energy assessment and retrofit planning towards cities' carbon neutrality, as requested by latest EU directives.

Intercepting a recognized gap in the literature, the use of thermography has been widened from surveys including single buildings – requiring the shooting of multiple pictures – to wide scale analyses with pictures recorded from the air, registering the infrared together with the visible bands with a high spatial resolution. Both raster and vector data were used, so that data derived from thermographic images enriched a shapefile of the volumetric units and their correlation with the EPC dataset has been investigated for extending the energy classification to all buildings and estimate the energy demand at district scale.

The approach has been tested and validated through a case study conducted in a district of Turin, Italy, one of the EU cities targeted to achieve carbon-neutrality by 2030. By also leveraging geometrical data to estimate the potential photovoltaic productivity of the available roofs, the method is used to outline and discuss potential retrofit scenarios that align energy demand and production with the goal of achieving carbon neutrality.

Section 2 provides information on the methodological aspects related to this study – from data acquisition to validation to return of final results – and introduces the case study. Section 3 presents intermediate and final results on the validation and testing of the new methodology for building energy classification and determination of energy demand and production. Section 4 discusses the results by delineating potential exploitation of the validated methodology in the assessment of alternative retrofit scenarios, while section 5 wraps up the study by providing conclusions and future perspectives.

2. Methodology

The methodology used in the present work can be schematised in three principal steps. Fig. 1 shows them for the two workflows of energy demand and production assessment, driving to the results and potential application phases.

In the energy demand assessment workflow, the first step is the image production, which entails orienting and georeferencing the thermographic picture acquired through aerial surveys. In the second step, volumetric units are identified and assigned an energy performance class, which is the first input for calculating the thermal energy demand. The other required data, such as the energy demand related to the different energy performance classes, the building heated surface, the number of resident people with the associated electrical uses, are gathered by questioning open data available in geographic systems, EPC database, or the literature, so that the total energy demand can be calculated.

In the production assessment workflow, the first step regards the elaboration of DSM, required in the second step to estimate the availability of solar radiation and therefore calculate the potential PV producibility after gathering data on PV performance.

The so-described methodology is designed to allow elaborating georeferenced results regarding energy demand and production on a GIS platform, which can be used to assess the impact of different retrofit scenarios in terms of primary energy and CO_2 emissions savings. In this study, an application to the city of Turin, Italy, is presented.

2.1. The case-study

The study area is part of the *Barriera di Milano* district, in Turin. It is a marginal area in the Northern periphery, characterised by strong social distress and physical degradation. It is bounded by key mobility infrastructures: an abandoned railway trench on the North (likely to host the second metro line of the city) and big avenues on the other three sides (Giulio Cesare, Vigevano and Venezia avenues from East to West). Moreover, two main roads cross it: Cigna street and Vercelli avenue. Fig. 2 shows the boundaries of the study area, reporting the main roads both bordering and crossing it. Moreover, the two red frames indicate the two principal clusters analysed in the following maps.

The area has a heterogeneous building stock, with a commercial area and a former industrial plant in a zone which is mainly residential. The history of the whole Northern part of Turin is characterised by a strong tie to the industrial sector. Most buildings were realised after World War II, following the pressing housing demand derived from the industrial boom. They were built in series with poor materials, often resulting in

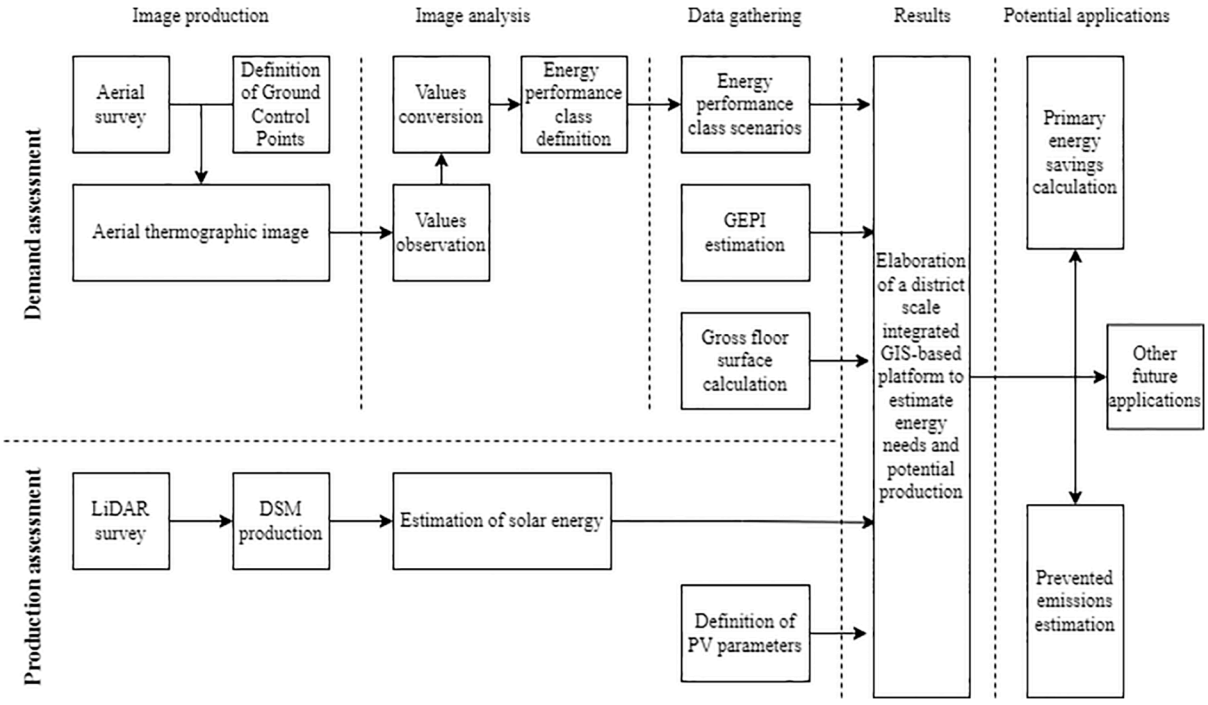

Fig. 1. The novel multi-step methodology proposed in this work.



Fig. 2. Definition of the study area.

inadequate energy performances. To mitigate the deriving impacts, there is the need to provide a wide-scale energy classification and an analysis of the potential benefits of a retrofitting campaign. Nevertheless, some buildings – mainly in the area of Cigna street – have good performance due to recent interventions.

Both main buildings and minor buildings – mainly garages and service buildings, according to the definition provided in (Decree, 2011) – were included in the analysis. The average height is equal to 2.17 floors, increasing to 2.83 when excluding the minor buildings from the count. Given that buildings have a bigger surface too, on average their gross floor area is 50 % higher than the one calculated considering all the volumetric units.

2.2. Photogrammetry: image data acquisition

Thermographic images were the first input for the evaluation of the thermal energy demand. The pictures used in this study were acquired between 12:39 and 13:25 on 9/1/2022 using the FLIR A8581 Compact MWIR HD thermal camera. This camera registers the bands in the range of 3-5 μm with a resolution of 1.3 MP and an accuracy of ±1 °C. The pictures were acquired at an altitude of approximately 1270 m.a.s.l. from a nadiral point of view so that only roofs could be observed. However, the high spatial resolution makes it possible to clearly distinguish disturbing elements – such as dormers and chimneys – so that they do not have influence on the results. Because of the acquisition timing – around midday –, accurate post-processing had to be performed to deal with the solar radiation, with the insulated pitches showing values considerably higher than the shadowed ones.

First, thermographic pictures were georeferenced to overlap them to volumetric units (i.e., one volumetric unit corresponds to a building, for which the energy demand was calculated), ensuring spatial consistency. For keeping the process as simple as possible, georeferencing was carried out in ArcGIS Pro, the same software which was used hereinafter. Ground Control Points are defined as points which can be identified also on an already georeferenced picture, which must have a spatial resolution equal to or higher than the first – not to reduce the accuracy. For this step, it was possible to use a precision orthophoto realised in the TerraItaly™ Metro HD project for the SDG11 Lab from Politecnico di Torino (SDG11 Lab), mapping the study area with a precision of 5 cm.

After the georeferencing process, it was calculated that the thermographic images covered an area of approximately 0.35 km^2 in three clusters. These include a heterogeneous set of buildings, with variability in terms of function, construction period and dimensions.

2.3. Image data elaboration for energy-related estimation

Once having localised the images, the first step consisted in the quantification of the envelope performance of the analysed volumetric units, based on the assumption that the temperature on the visible building surfaces (the roofs) is an indicator of the thermal losses through the building envelope, which is the main driver for the building energy classification of existing buildings. Three operations were required for this step: 1) the definition of the largest possible shadowed area for the ceiling of each volumetric unit – shadowed pitches were taken into account to minimise the errors deriving from direct solar radiation and other localised defects –, 2) the clip of the thermal image with the defined area and 3) the calculation of the average pixel value for each of the resulting files, leading to determine an average temperature value for each roof. The process was iterated in the GIS environment for the entire set of 430 analysed units.

The entire process from raw data gathering and elaboration to the resulting energy performance classification is reported in Fig. 3 for a sample building block of the district. The upper line shows how the surface temperature values – returned by the thermographic picture – were aggregated for volumetric unit, ordering them progressively in a spreadsheet to enable the classification in the next step, based on the integration with data from available EPCs.

The lower line of Fig. 3 reports the process related to the analysis of EPC data, gathered from the regional database. The analysis was based on the most recent EPC for each volumetric unit that could be

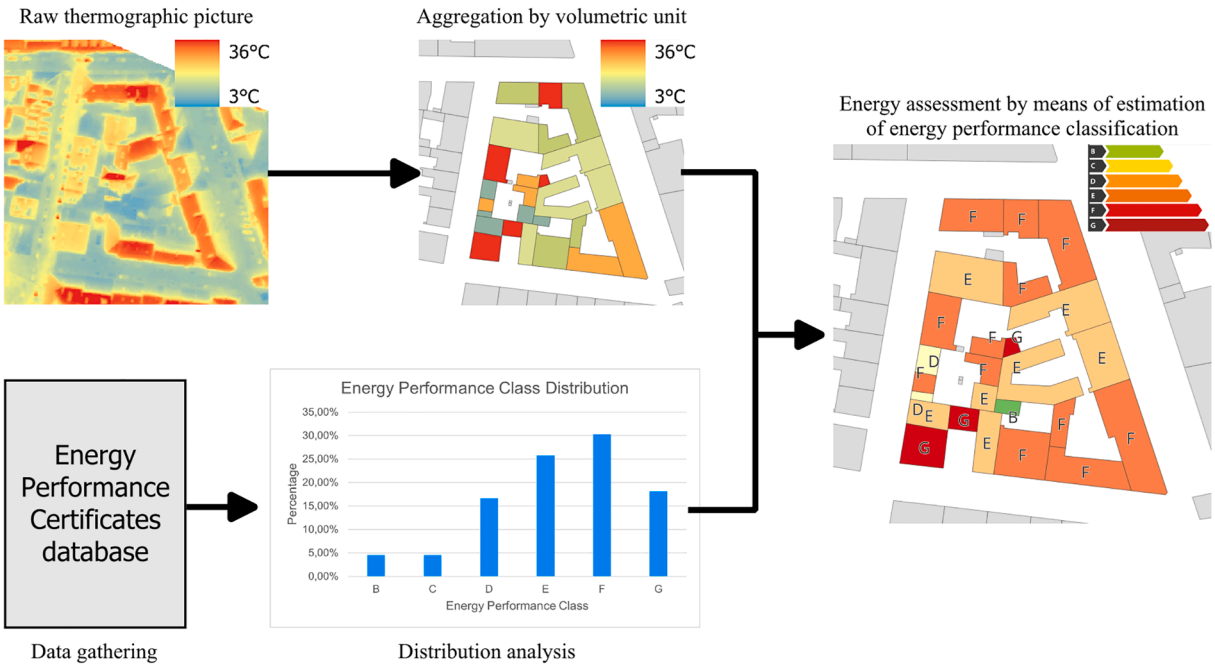

Fig. 3. Visualization of the workflow for the attribution of the energy class.

downloaded from the IT system of the Piedmont region, gathering a total of 66 of them for the case-study area. The distribution of energy performance classes in the district was then derived, as shown in the graph of Fig. 3, showing that the greatest share is accounted for lower performances, where the three least performing classes strongly outnumber the most performing ones. The obtained distribution curve was then replicated to extend the analysis to the whole district. In fact, all buildings in the district were ordered in a spreadsheet according to their average roof temperature resulting from previous steps, and then correlated to an energy performance class according to the previously obtained distribution of classes, allocating to each class the corresponding share of volumetric units. Therefore, a linear regression model was used, assuming the class distribution of the analysed set of buildings as directly following the trend in class distribution in the training dataset.

Data from the existing EPCs database were then used to define a Global Energy Performance Index (GEPI) for each class. The GEPI quantifies the non-renewable primary energy consumptions in the case of a pre-defined standard use of the building unit. It consists in the sum of the energy needs for heating and cooling, domestic hot water (DHW) production, ventilation and – for non-residential buildings – for artificial lighting and internal movements of people and goods, for which the calculation method is standardised in Italy in UNI/TS 11300 (UNI, 2019) standard series. These parameters were extracted from the EPCs, regulated in Italy by the Legislative Decree 192/2005 and following integrations (Decreto Legislativo, 2005), which report the energy performance classification deriving from calculations performed according to the UNI/TS 11300 standard, thus providing a method to compare the performance of different buildings under standard and uniform assumptions. For buildings in the area, it can be assumed that GEPI only includes primary energy for heating and DHW uses, since most buildings in the area are residential and do not have a cooling nor a ventilation system.

In the current regulatory approach for building energy classification, also due to possible differences in the energy supply systems, it may happen that a building characterized by a lower absolute GEPI value is assigned to a higher energy performance class and vice versa. Therefore, in order to limit the impact of extremes, it was decided to adopt the median value rather than the average as the reference value for energy consumption to be attributed to each energy performance class. As shown in Table 1 – where the two values are compared for each energy class – this has not led to an overestimation nor underestimation of the consumptions: in three cases the median is higher than the average and in the other three it is lower. However, median values constantly increase, differently from the average for which class D buildings consume more than the ones classified as E. The interval between the values is not constant, but rather maximum in the lower classes and very limited in the central ones. In particular, class G requires approximately 100 kWh/m^2 more than class F, while only 15 kWh/m^2 divide classes C and E.

Based on the relevance of energy classification on the following results and considering the correlation between thermography and energy performance class as the core of the research, validation was required to test the reliability of the results. As mentioned above, only one EPC was taken for each volumetric unit, if available, leaving the other EPCs as a test set to check the reliability of results and therefore validate the methodology. Results are to be assessed in terms of variance between the estimated energy performance class and the actual one – returned in the EPC used for validation –, considering acceptable that differences do not exceed two classes, with the possibility of increasing the accuracy by entering more training data in the calculation model. The validation process is shown in Fig. 4 for the sample building block, where the energy performance classification resulting from the process explained in Fig. 3 is compared to the actual energy performance classes of control units included in the EPCs test set.

Table 1
Reference values adopted for the GEPI of each energy class.

Energy class	Count [-]	Average GEPI [kWh/m^2]	Median GEPI [kWh/m^2]
B	3	86.33	98.06
C	3	117.95	118.95
D	11	146.27	123.15
E	17	143.11	130.49
F	20	174.35	176.24
G	12	293.79	276.22
Total	66	160.30	153.85

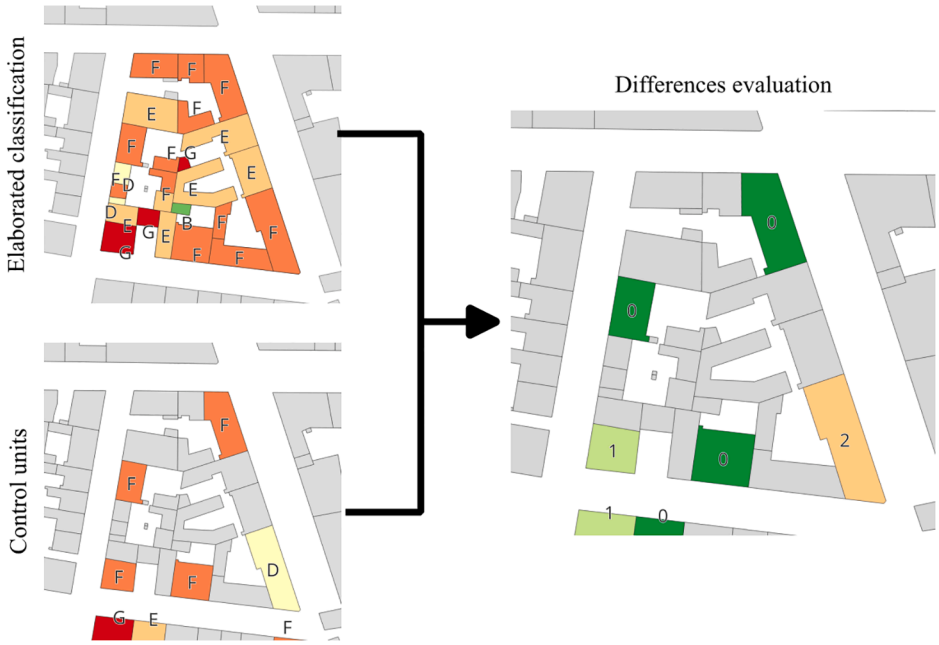

Fig. 4. Visualization of the validation workflow.

2.4. Definition of current energy demand

After quantification of the specific primary energy consumptions for each energy performance class, deriving from the interpretation of the thermographic images, the calculation of the overall energy demand at district scale is subject to the determination of the heated surface area for each building unit. The gross floor area is calculated by multiplying the footprint area by the number of floors. Although the input values were provided in the volumetric units file, some fields required additional calculations due to errors in the database entries. When values were missing, the number of floors was calculated by dividing the unit's height by 3.3 metres – the estimated average height of each floor based on construction period. This approach simplifies the calculation as the real height varies depending on the building's function– for instance, residential rooms are typically lower than industrial spaces. Additionally, only habitable attics were included in the count of floors since they are heated (as also confirmed by thermographic images).

Considering the prevalence of natural gas boilers as heating and DHW supply systems emerged from the analysis of EPCs, the district thermal energy consumption Q_{H+DHW} was calculated as follows (Eq. 1):

$$Q_{H+DHW} = \sum_{i=1}^{n} \frac{GEPI_{class,i} * GFA_{i,heated}}{f_{pe,\ gas}} \quad [\text{kWh}] \tag{1}$$

where $GEPI_{class,i}$ is the GEPI related to the energy performance class of the i building, $GFA_{i,heated}$ is the heated gross floor area of the i building, $f_{pe,\ gas}$ is the Italian non-renewable primary energy conversion factor for natural gas (set to 1.05) and n is the number of buildings included in the district of study.

The electrical energy demand for residential buildings (referring to other energy uses not involved in the GEPI) was also calculated based on estimation of electricity consumption per capita (1113 kWh/year (ISTAT)) and population density, derived from national statistical data (ISTAT).

2.5. Estimation of potential PV production

In the perspective of retrofit strategies towards electrification, the photovoltaic potential was also estimated. Indeed, photovoltaic panels are the most suitable renewable energy source to be installed in a densely built environment, based on the possibility to integrate them directly on the roofs.

The Suri equation was used for the calculation of the photovoltaic producibility. One of the parameters requiring a preliminary estimation is solar energy, which was esteemed through the ArcGIS Pro tool Area Solar Radiation. The key input is a Digital Surface Model (DSM) for the area of analysis: it was used the DSM produced through the LiDAR points registered during the flight for the TerraItaly™ Metro HD project; when using a georeferenced file, the latitude is automatically set. The default "sky size" of 200 was used, while for the "time configuration" it was chosen the "whole year" option, analysing year 2022 with a day interval of 14 days – set by default – and an hour interval of 1 hour. Finally, the "create outputs for each interval" option was checked: the output raster would contain one band for each of the set time intervals. Further parameters are grouped in two clusters.

- Topographic parameters: the "z factor" was kept by default, 1, because planar and vertical units use the same unit of measure and scale. The "slope and aspect input type" was calculated "from the input surface raster" – the DSM – and the "calculation directions" were reduced from the default 32 to 16 to speed up the process.
- Radiation parameters: zenith and azimuth diffusions were kept by default, 8 each, while the "diffuse model type" was changed into "standard overcast sky", with the diffuse radiation flux varying with the zenith angle.

Two other parameters, named diffuse proportion and transmissivity, had to be set to adapt the study to the atmospheric conditions of the test site and change depending on the period of the year. The former was defined through PVGIS (European Commission, 2023), an online tool created by the European Commission which calculates monthly data of

Table 2
Diffuse proportion and transmissivity parameters used for the estimation of solar energy.

Season	Diffuse proportion [-]	Transmissivity [-]
Winter	0.38	0.56
Summer	0.38	0.76
Spring/autumn	0.42	0.67

the global horizontal radiation in a user-defined location. The latter was calculated based on inputs from the same tool and pre-defined parameters (the LINKE turbidity factor and the solar constant). The elaboration required nearly two hours to finish, so the trade-off between good accuracy and efficiency was to define three seasonal averages. The resulting values are reported in Table 2.

The output of the Area Solar Radiation tool is a raster. To make its values usable, it was converted into points, which were then attached to the volumetric units.

Once having obtained a reference solar energy value for each unit, the photovoltaic potential was calculated as in Eq. 2 (Suri equation):

$$PV_{potential} = \text{Solar energy} * PI * \eta * \text{surface} \ [\text{kWh/year}] \quad (2)$$

The Performance Index (PI), which indicates the efficiency of the system, was assumed to be 75 %. The conversion efficiency (η, ratio of electricity produced out of the incident solar energy) was defined according to Green et al. (2022) – 24.2 % for crystalline cells, 18.4 % for multi crystalline and 11 % for thin film. The surface was considered as 40 % of the building footprint, with this value balancing between the surface reduction given by the incorrect orientation of some pitches and the increase resulting from the inclination. The surface correction factor is extracted from Vecchi (2022), where different studies are compared on the computation of the usable rooftop area: Pelland and Poissant (2006) adopted the 40 % value, while other authors as (Hofierka & Kaňuk, 2009, Gagnon et al., 2016, Odeh & Nguyen, 2021) considered up to 66 % of the footprint to be exploitable. On the other hand, Bergamasco and Asinari (2011) used a series of correction factors resulting in less than 10 % of the overall building footprint to be considered as exploitable: for the purpose of our study, the 40 % value emerged as a good average between the extremes.

2.6. Definition of retrofit scenarios

Once having established and validated the methodology for the energy performance classification of buildings and estimation of energy demand and production potential at district scale, it can be exploited for future scenario analysis, by looking at the variations of results when changing some of the input parameters. The scope of this step is to test and discuss its potential to support and drive future energy policies, which should find an optimum that maximises energy savings while minimising investments.

In this study, two scenarios were considered with a view on the EU targets for building decarbonisation.

The first scenario aims at achieving the re-classification of all the buildings in the most performing class, thus acknowledging the potential savings achievable with structural interventions only. The second scenario, which involves an improvement of at least two energy classes, aligns with recent renovation policies in Italy that have set this threshold as a requirement to access incentives. Also, this scenario takes into account the minimum requirements set by the new EPBD, which mandates the upgrade of all buildings to at least class D in 2033.

Considering that a same energy class upgrade can be achieved combining measures aimed at reducing energy demand and measures aimed at increasing the efficiency of energy systems, the estimation of potential savings of primary energy and CO_2 emissions for the two main scenarios was performed considering different alternatives that are feasible in the short-term:

1. the upgrade in energy classes is mainly obtained by improving the envelope performance, while leaving the current situation where most buildings are heated through natural gas boilers;
2. the upgrade in energy classes is obtained after the implementation of the so-called Project North-East by the City of Turin, through which the study area will be provided with district heating;
3. a hybrid scenario where natural gas boilers and district heating coexist, accounting for 50 % each.

In all these three cases, the electricity is taken from the network, without any form of auto production. However, in the perspective of creating renewable energy communities at district scale, we also considered

4. an electrification scenario, where heat pumps are used to provide thermal energy and the required electricity is provided by renewable energy produced by PV.

The non-renewable primary energy conversion factors for natural gas and electricity from the grid are set – respectively – to 1.05 and 1.95, as defined by the Italian Ministerial Decree 26/06/2015 (Ministri dello Sviluppo Economico dell'Ambiente e della Tutela del Territorio e del Mare delle Infrastrutture e dei Trasporti per la Semplificazione della Pubblica Amministrazione 2015). The emissions factors for natural gas and electricity were set, as defined in Koffi et al. (2017), to 240 g_{CO2}/kWh and 424 g_{CO2}/kWh.

The parameters for district heating are published yearly by the service provider (IREN in the case of Turin, which delegated the calculation to Rina Services S.p.A.). In this study, we have set the 2022 data which indicates 165.2 g_{CO2}/kWh and 0.884 as emission and primary energy conversion factors, respectively (IREN Energia, 2021).

3. Results

Considering the interest in the methodology itself rather than just the final results, it is relevant to decompose the methodology by showing the outcomes of the principal phases. The following sections also explain the results of the intermediate calculations to make them explicit and show the input parameters that can be varied to assess the renovation scenarios.

3.1. Elaborated data resulting from thermal images analysis

First, it is relevant to analyse the range of temperature values that can be observed through the thermographic images. The pictures were acquired around midday on a winter day, temperatures range from approximately 3 °C to 36 °C. As expected, the highest values were recorded for the roof pitches in the sunshine made of good conductors, such as metals.

Fig. 5 shows the elaboration of the thermographic pictures. They are provided individually in grayscale, with a bar indicating the temperature corresponding to each pixel value. ArcGIS allows the user georeferencing and representing them in false colours to show the temperature variations, overlapping the common points.

As previously explained, only the shadowed parts were recorded, resulting in a reduced temperature range between 3 °C and 22 °C (from 0.428 to 151.205 in Digital Number), to which the different energy performance classes were correlated as explained in Section 2.3, resulting in the class delimiting thresholds reported in Table 3. On average, there is a difference of 3.55 °C between two subsequent classes. The highest difference can be observed between classes F and G, with 7.7 °C separating the two, while 0.78 °C only separate the two most performing classes.

As shown in Fig. 6, showing the placement of the volumetric units of the six energy classes in the area, it is difficult to find out a pattern in the spatial distribution of the energy classes, with a substantially even diffusion. Still, there are some exceptions. The complex of the former Gondrand plant is composed of constructions with high dispersion: the main warehouse falls in class F, while other buildings are in classes E and G. On the contrary, the westernmost area, comprised between Venezia avenue and Cigna street, is characterised by the presence of some of the most high-performing buildings. The densest area is also the most heterogeneous: constructions of all classes are gathered around Vercelli avenue, despite the prevalence of low-performing units.

The class distribution can be analysed also in terms of the total gross

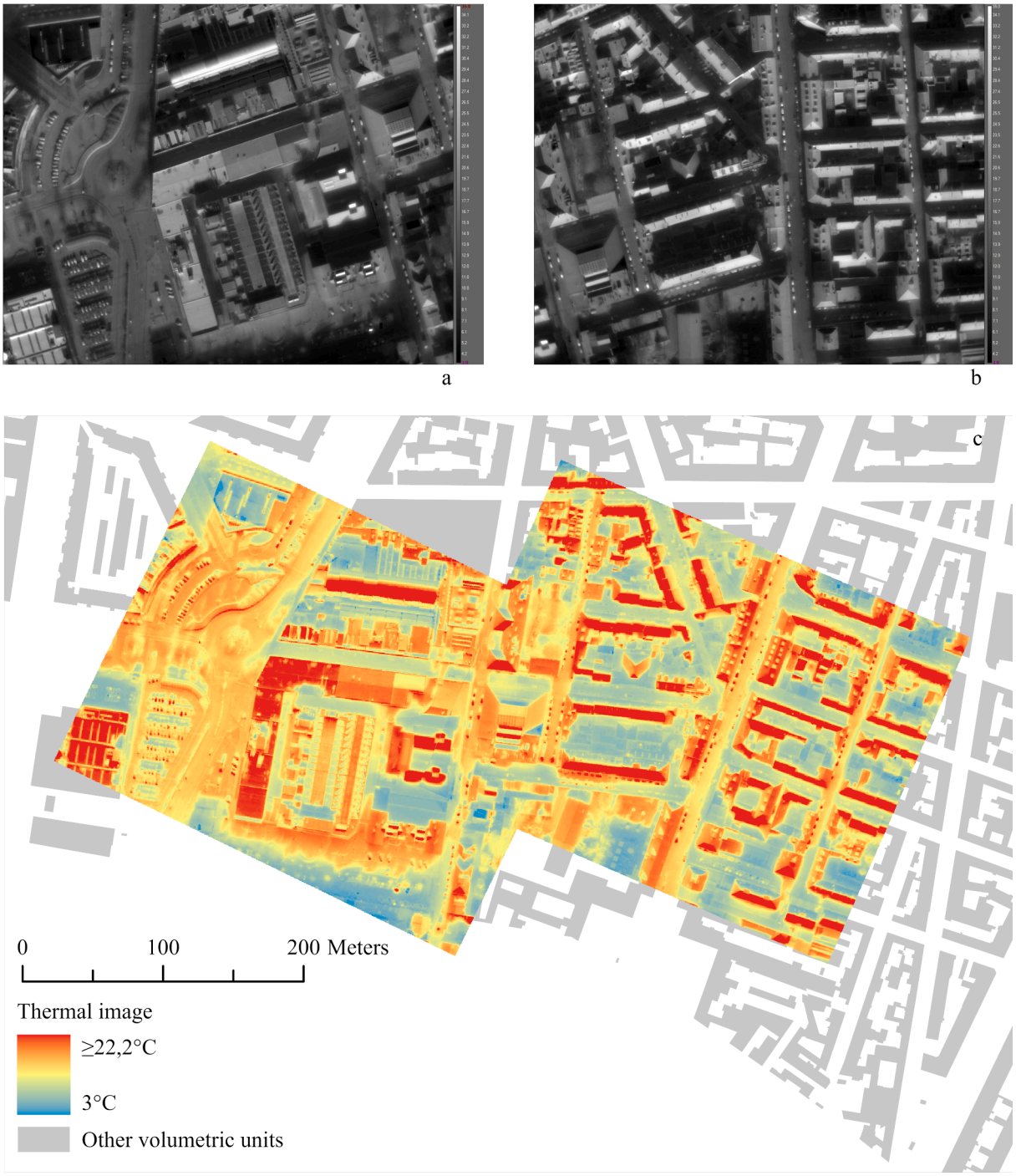

Fig. 5. Example of thermal images before (a and b) and after (c) post-processing.

Table 3
Correlation matrix between temperature and energy performance classification.

Energy class	DN threshold [–]	Temperature threshold [°C]	Count [-]	Share [%]
B	14	4.81	20	4.65 %
C	20	5.59	20	4.65 %
D	37.12	7.80	72	16.74 %
E	64	11.28	110	25.58 %
F	91.8	14.88	130	30.23 %
G	151.21	22.57	78	18.14 %

floor area of the units included in them. The area increases constantly from B (131 m^2) to F (935 m^2) with an interval which overcomes 220 m^2 in all but one case – from D to E it increases by 64 m^2 only. Class G buildings have a significantly lower surface to be heated, 336 m^2, with these data mitigating their impacts resulting from high consumptions. Similar trends can be observed considering the building footprint.

Results were validated with a dataset of 25 EPCs not previously included in the calculation. Based on the concurrent need to select a random sample and to test the reliability of the pictures in the whole area, 25 sub-zones were identified, taking one EPC for each of these sub-zones. The energy class reported in the EPC was compared to the one returned by the calculation model, then accessing the discrepancies

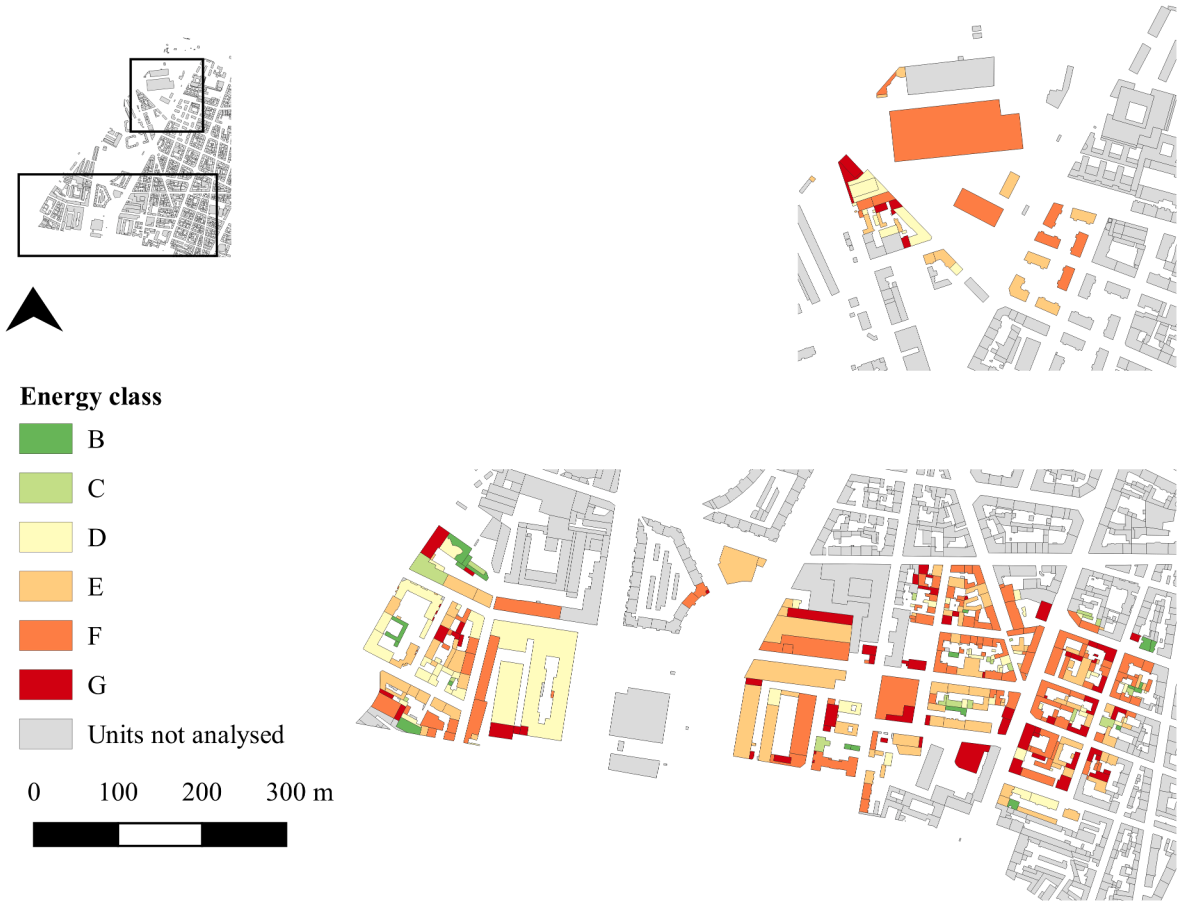

Fig. 6. Energy performance classes of buildings resulting from integration of EPC data and thermal images elaboration.

between the output of the proposed method and the validation data. The results proved to be sound, meeting the expected criteria and the accuracy levels of previous studies. In the test set, 100 % of the units did not differ by more than two classes in terms of energy performance. Additionally, 76 % of the test set exhibited a difference of one class or less, out of which 80 % were exactly classified.

As this is a multi-class classification problem, it is possible to assess the reliability of the model by considering the Receiver Operating Curve (ROC), which compares the True Positive Rate and the False Positive Rate by plotting them in a dispersion graph (Fig. 7), with the One-vs-Rest scheme. By comparing the macro-average – used to better report the global performance of the model – of the classification performed using the full dataset (66 EPCs) and a subset (40 EPCs randomly selected inside the full dataset), it is immediately evident that – despite both of them provided acceptable results, better than the chance level (with AUC equal to 0.5) – the model clearly improves by adding training data. Indeed, the classification with 40 EPCs has an AUC equal to 69 % of the AUC of the full classification. By increasing the number of training data, the effectiveness of the model is increased, with the ROC shifting to the upper left part of the graph – showing a sounder classification. This underlines the great potential of scaling up the model for improving the performance of the classifier, to be applied to larger city areas.

With these premises, it was possible to compute the energy demand of the overall district.

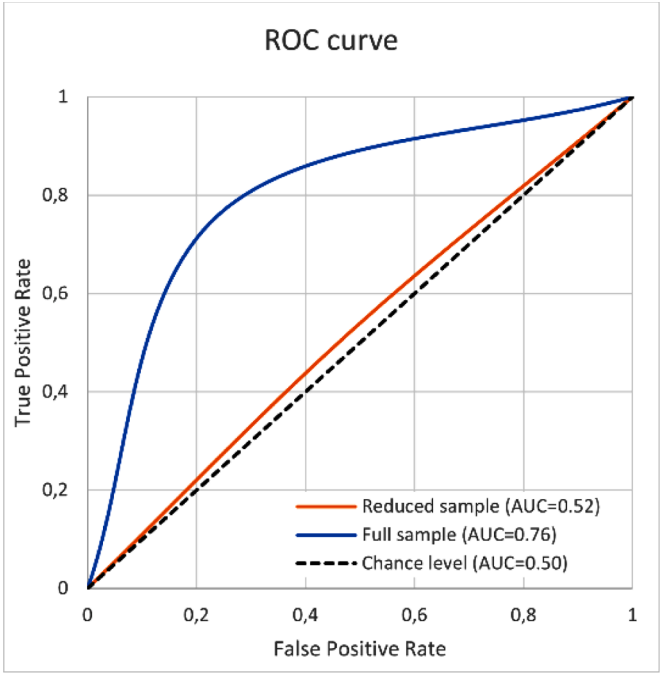

Fig. 7. ROC curves for the full training sample and a reduced training sample.

3.2. Energy demand and performance assessment

To provide a general assessment of the building stock, raw data about single volumetric units can be aggregated. The total thermal energy demand of the district amounts to 42 GWh/year, corresponding to 155 kWh/m^2. Therefore, it could be stated that currently the average building in the area of interest can be classified as a class E, with little improvements – around 12 kWh/m^2 – needed for a class upgrade.

As mentioned in paragraph 3.1, there are high variations in the amount of heated floor area in each class. This parameter strongly influences the variations in the energy demand, because of the reduced deviation between consumption values – especially for the central classes.

The less demanding units are the smallest, generally located inside blocks, while the former industrial buildings located in the Northern part of the study area are the most consuming. In particular, the extremes are a small laboratory (minor building) requiring just 141.67 kWh/year and the principal shopfloor of the industrial area, requiring 7.5 GWh/year alone. The most common range is the one which includes volumetric units requiring between 10 and 100 MWh/year. Buildings with these characteristics are located especially in the South-Eastern area – the one characterised by a dense and homogenous stock.

As for the electricity demand, 161 volumetric units are partially or totally residential and therefore consume electricity for domestic use. The consumptions range from 1113 to 107961 kWh/year, with the population ranging from a single person to 60 residents. On average, every residential building consumes 19460 kWh/year, totalling approximately 3 GWh/year. Also because of the prevalence of gas boilers as energy systems, the electricity demand accounts for 9 % only of the total energy demand. Still, it has to be considered that, at the moment, the impacts of using electricity from the grid is considerably higher compared to the other energy vectors in terms of both primary energy and CO_2 emissions, unless electricity is produced from renewable energy sources.

Fig. 8 shows a classification of the volumetric units based on their total energy demand. Based on the low share of the electricity demand over the total, this outcome is comparable to the one about thermal energy demand. The most energy intensive buildings are the biggest ones – former industrial or commercial – while the less demanding are generally the minor buildings located inside the courts.

3.3. Energy production assessment

Fig. 9 quantifies the amount of available solar energy in the same area in the months of December and August. Considering that solar energy is one of the principal parameters influencing photovoltaic production, it is interesting to note that there is high variability. Apart from the difference in production, given by the sum of multiple factors during summer – better weather conditions resulting in less diffused radiation, more hours of light and more intense radiation –, a strong dissimilarity between seasons depends on solar height. While during winter the roofs emerge as the only surfaces stroke by relevant solar radiation values, in summer also roads (at least the biggest ones) show high radiation values overall.

Approximately 8.8 GWh can be produced yearly by installing polycrystalline photovoltaic panels on the roofs of the district. Values range from less than 1 kWh to more than 1 GWh produced for a single volumetric unit. Among the buildings producing more than 120 MWh/year, the one with the smallest footprint is 1200 m^2 wide. As expected, the largest buildings are often the ones with the highest productivity. Indeed, thanks to their nature – as former industrial buildings or wide commercial places – they can take advantage of a wide sun-exposed surface without any shadowing elements. This can be observed in Fig. 10, which classifies volumetric units based on the potential production.

Compared to polycrystalline, monocrystalline cells can produce the same amount of electricity occupying a lower surface – or produce more with the same installed panels surface. On the contrary, thin film panels

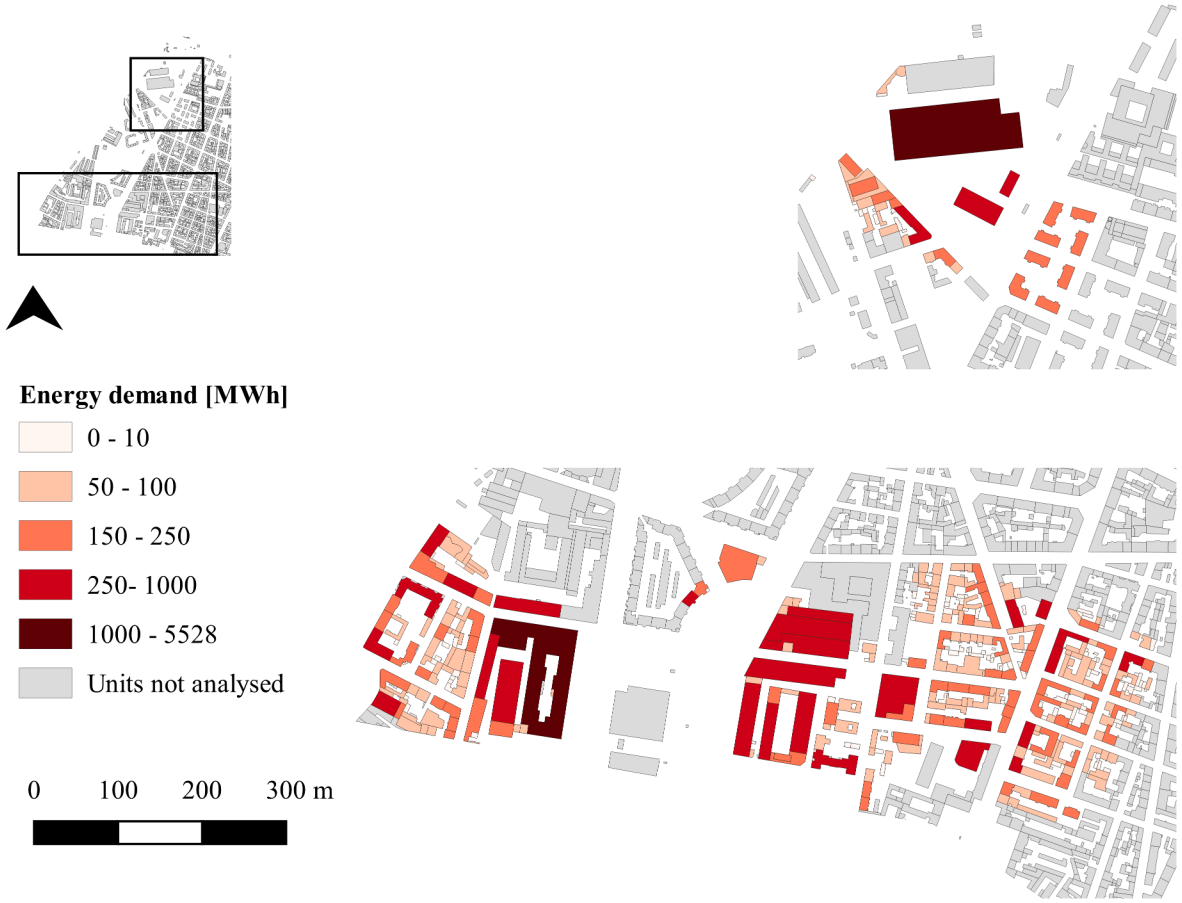

Fig. 8. Energy demand of buildings.

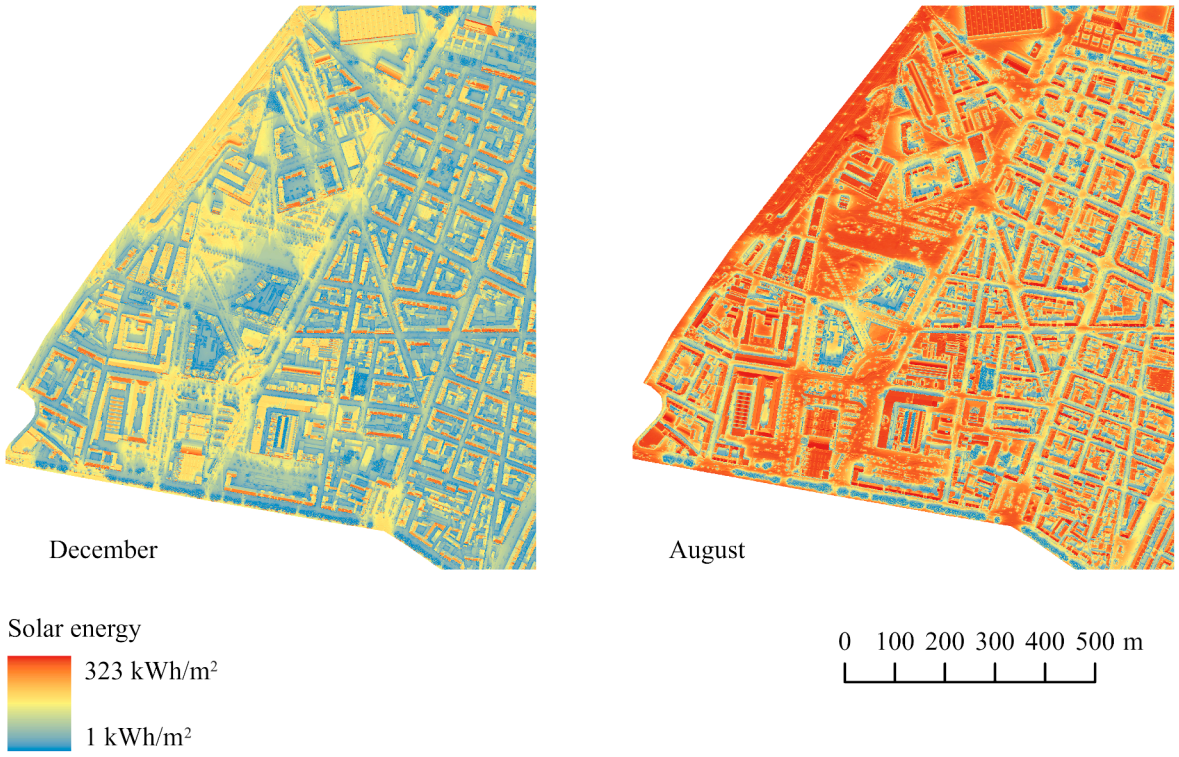

Fig. 9. Monthly solar radiation (December – August).

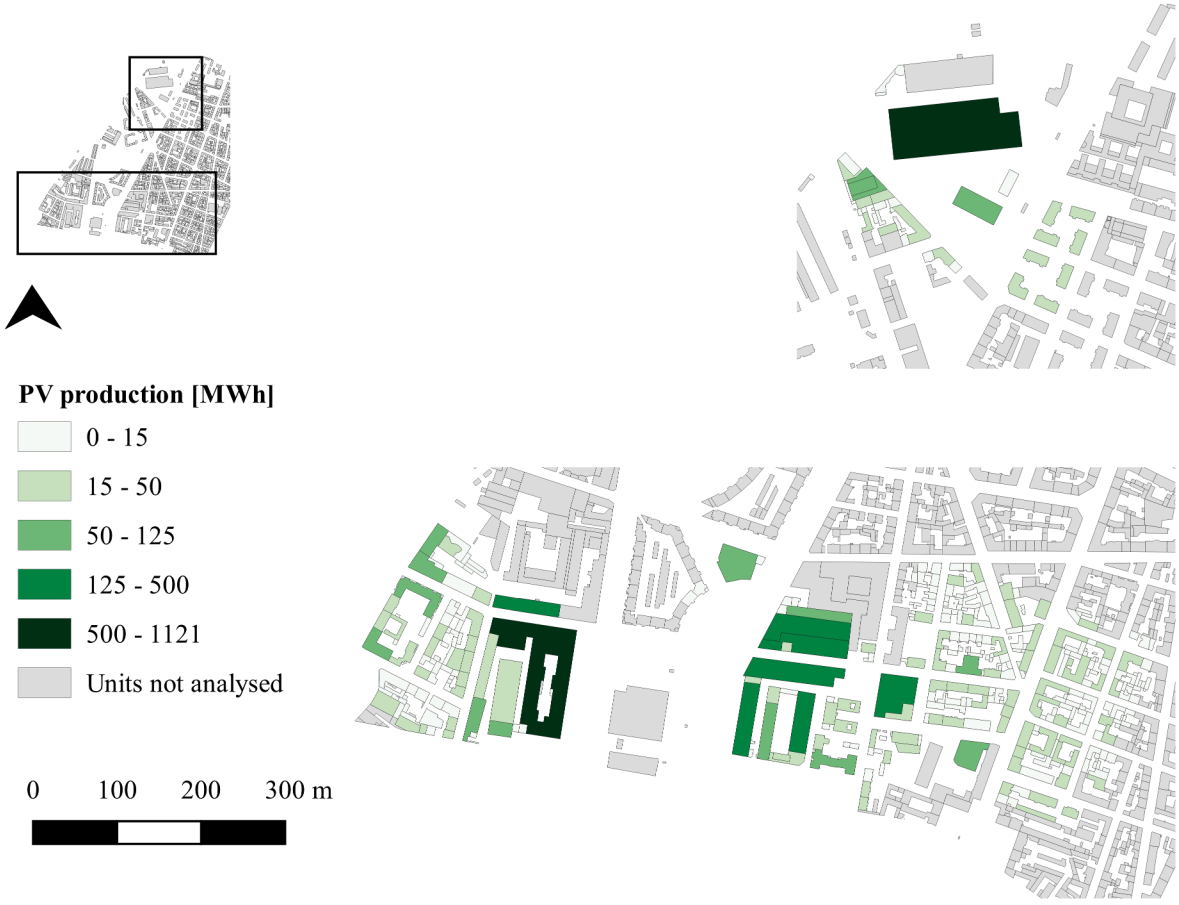

Fig. 10. Estimation of annual PV energy production potential.

are less efficient, but they are also cheaper. A careful analysis relating investment costs to the benefits is required to shape the ideal configuration for auto production.

The potential production was related to the esteemed consumptions in Fig. 11, where the share of electricity demand which can be met through polycrystalline panels is indicated. Slightly more than half of the units can produce by themselves the electricity needed to fulfil their demand, with 24 units (15 %) producing more than twice and 6 more than five times their needs. These extremes cause the average ratio between production and consumption to raise to 135 %. Nevertheless, the selected sample can produce less energy than its need, 83.20 %.

Compared to polycrystalline, monocrystalline cells can produce the same amount of electricity occupying a lower surface – or produce more with the same installed panels surface. On the contrary, thin film panels are less efficient, but they are also cheaper. A careful analysis relating investment costs to the benefits is required to shape the ideal configuration for auto production, but the present results are promising. Furthermore, in the current scenario, it is possible to foresee collaboration forms by which residential buildings take advantage of the panels installed on other roofs. By doing so, it would be possible to produce in the district 279 % of the current electricity need, paving the way to renewable energy communities and highlighting the feasibility to cover the additional electricity needs caused by building electrification.

4. Scenario analysis and discussion

In the following two paragraphs, it is discussed how the resulting methodology can be used to assess different renovation scenarios at city scale. To do so two examples of alternative scenarios are compared: the first refers to a reclassification of all buildings in class B, the second to an upgrade of two classes, as detailed in Section 2.6. Both main scenarios are assessed considering four alternative energy supply options (therefore implying different combination of reduction of energy needs and increase of system efficiency to reach the targeted class), namely District Heating (indicated as DH), natural gas (G), a mix of district heating and natural gas (M) and heat pumps, where part of the electricity demand is covered by photovoltaic production (HP+PV).

4.1. Retrofit scenarios

The first analysis concerned the savings in terms of primary energy. Fig. 12 shows, for the current state and the two retrofit scenarios, the yearly savings quantified in GWh. In the current situation, natural gas is

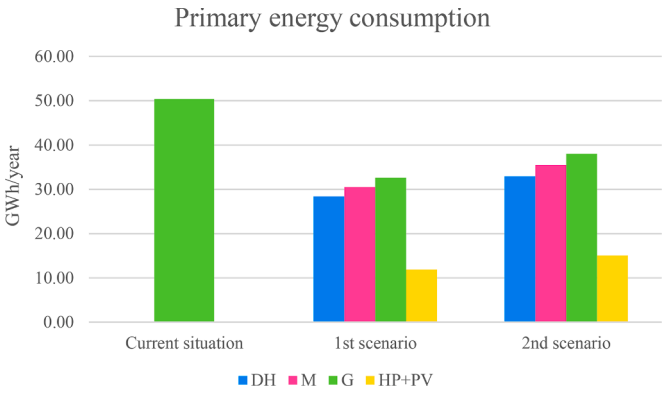

Fig. 12. Non-renewable primary energy consumption.

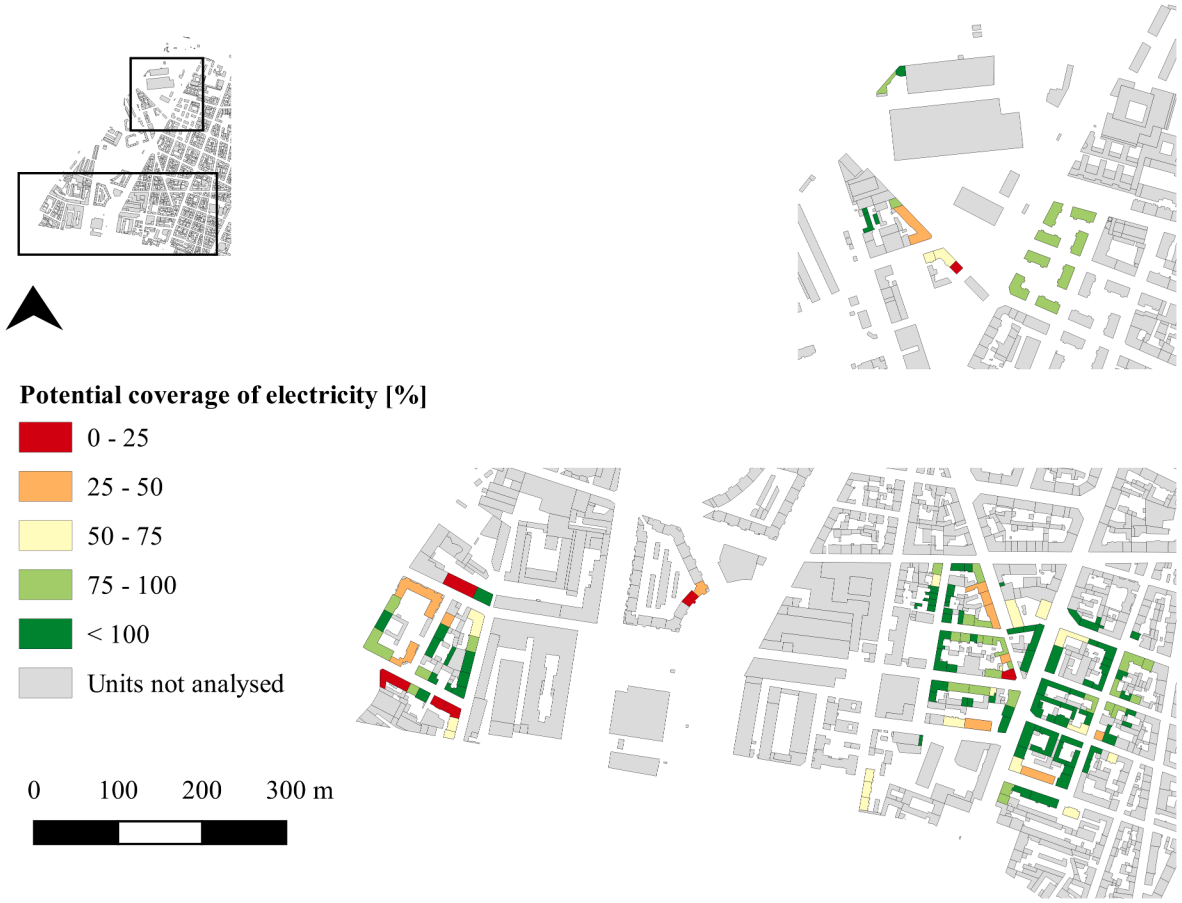

Fig. 11. Potential annual coverage of estimated electric consumptions (current state).

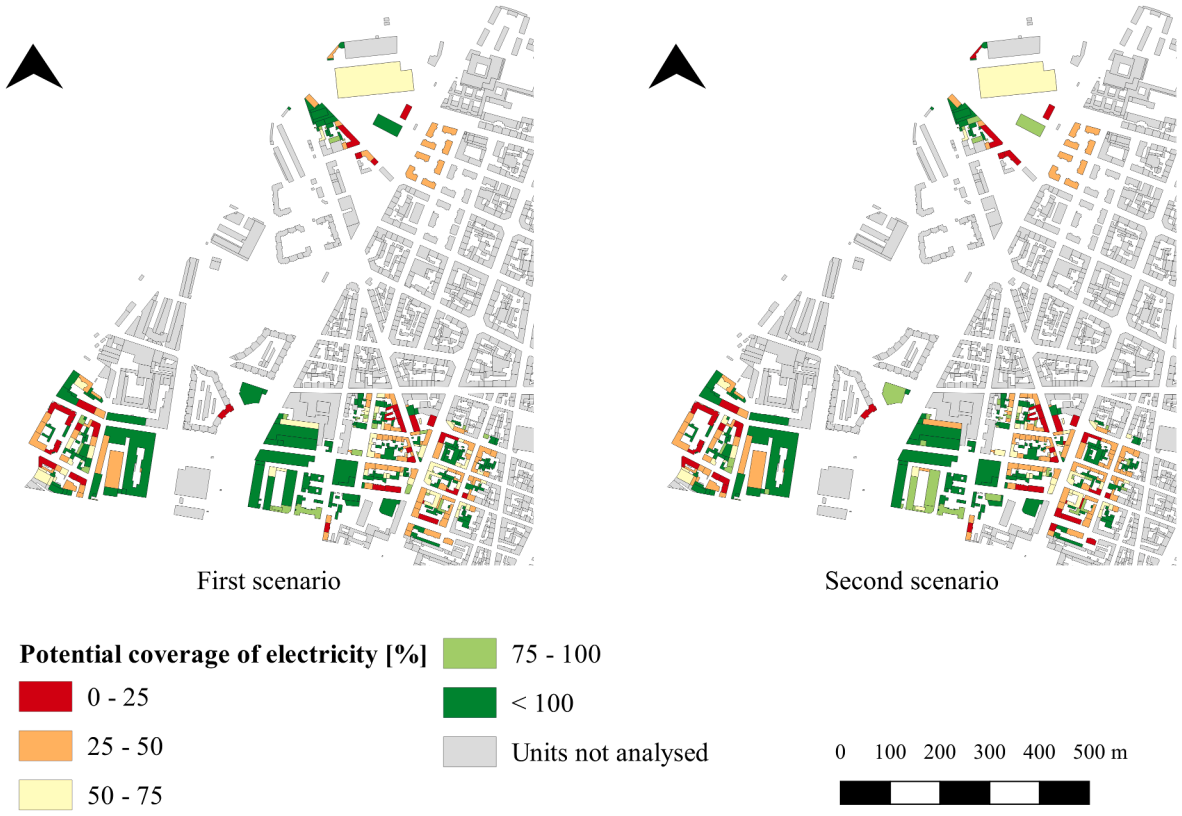

Fig. 13. Potential annual coverage of estimated electric consumption (future scenarios).

the only energy supply option. Keeping natural gas boilers in the whole building stock even in the case of a renovation would be the most energy intensive solution, with the possibility of doubling the savings when installing heat pumps and self-producing part of the energy through photovoltaic panels. On the other hand, district heating – likely to be introduced in the district in the short-medium term – grants savings more than 15 % higher compared to natural gas.

In the first scenario, with all the buildings classified in class B, the total energy demand would be reduced by at least 35.27 %. Nevertheless, the implementation of the district heating grid would save additional 4 GWh of primary energy yearly. If heat pumps and self-production are implemented, primary energy demand is reduced by ¾. A relevant share of these savings could be obtained by upgrading the most intensive energy buildings, the mentioned former industrial plant, with primary energy savings ranging between 3.48 and 6.78 GWh. On average, between 41 and 89 MWh can be saved in each volumetric unit.

The second scenario, which is the most likely one to be implemented to comply with the new EPBD requirements, would result in approximately 26 % of units being included in the highest performing class. This represents a five-fold overall district performance increase compared to the current situation. Therefore, the energy consumption would decrease at least by 24.56 % - 12.38 GWh in absolute terms. Nevertheless, it was mentioned that alternative energy configurations would result in higher savings, up to 70 % (35.29 GWh in absolute terms).

The second scenario could also be considered as an intermediate step before moving on to the first scenario. It offers significant benefits while still allowing room for further improvements in the building stock. In this intermediate step, without changing the energy vector, savings ranging from 14 % to 21 % can be achieved. However, the significance becomes even more apparent when considering a first upgrade in the short term, prior to the full implementation of district heating in the medium term (additional savings of 9.6 GWh in DH configuration), followed by complete electrification and renewable production in the long term (additional savings of 26 GWh in case of HP+PV configuration).

Moreover, this last scenario could be further improved considering that only half of the volumetric units can provide their electricity demand with photovoltaic panels. In particular, Fig. 13 – relating potential PV production and the electricity demand in the two future scenarios with HP+PV configuration – shows that 49.4 % of the units in the first scenario and 53.6 % in the second need to take part of their electricity needs from the grid. On the other hand, the self-sufficient buildings can produce a surplus equal to 1.63 GWh and 1.21 GWh – respectively in the first and second scenarios. Still, the deficit of the non-autonomous units amounts to 5.94 GWh and 6.54 GWh in the two scenarios, respectively. Therefore, it would still be necessary to keep the district connected to the grid unless further renewable energy sources or higher efficiency panels are installed in the area.

4.2. *Decarbonisation potential*

In Turin, the residential sector causes 37.2 % of the total carbon dioxide emissions. Since 1991, CO_2 emissions were reduced by 47 %, with the residential sector decreasing its emissions by 65 %. The target is to achieve climate neutrality by 2030.

Fig. 14 compares the current carbon dioxide emissions to the ones of the investigated retrofit scenarios. The scenarios are on the x axis, while the y axis quantifies the emissions in terms of tonnes of equivalent CO_2. Looking at the general outcomes of the comparison between alternative energy source configurations it can be observed that, similarly to trends related to primary energy savings, emissions are much lower when considering the use of heat pumps and photovoltaic panels (59.53 % and 56.59 % of emission savings in the 1st and 2nd scenarios, respectively).

In the two scenarios, emissions savings range between 24.71 % (G option, 2nd scenario) and 73.89 % (HP+PV option, 1st scenario). This would mean preventing emissions of at least 2829 tonnes of carbon dioxide, with the possibility of further halving the emissions through a transition to district heating, up to 8460 t if the first scenario is adopted

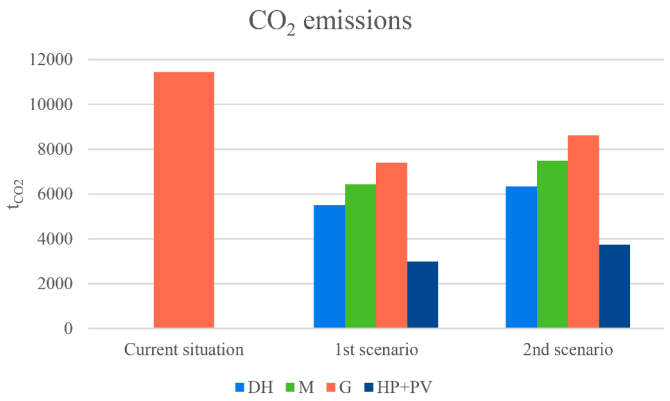

Fig. 14. Equivalent CO_2 emission in different scenarios (GB, M, DH, HP+PV).

together with heat pumps.

Compared to the savings quantified in primary energy, there are various gains in proposing additional interventions to couple an upgrading from the second to the first scenario with a change in the energy vector. Indeed, savings are 10 % higher in the case of a transition towards district heating and 6 % with a mixed scenario. On the contrary, considering heat pumps the gains are 3 % lower.

5. Conclusions and future developments

This article focused on the exploration of an innovative method to provide a comprehensive energy demand and production assessment and planning on a district scale based on integration of existing EPC dataset with high spatial resolution data acquired through aerial thermography. The research aimed first at providing energy performance classification of all buildings in the district, then defining the current energy demand – both thermal and electrical – and the potential electricity production with photovoltaic panels. Second, the potential savings from two retrofitting scenarios were evaluated based on the primary energy and the prevented emissions. In this phase, alternative energy supply options implying the use of different energy vectors were compared in terms of related primary energy consumptions and CO_2 emissions.

The results discussed the benefits and burdens of different scenarios implying different strategies in terms of building retrofitting and energy supply. The second scenario – in which all the buildings are upgraded by two classes, envisioning the measures proposed in the new EPBD recast proposal – appears to be a good trade-off between investment costs and potential benefits. Compared to the first scenario – implying all the buildings meet class B requirements – the benefits are approximately 8.5 % lower for both CO_2 emissions and primary energy consumption. On the other hand, there is the potential to install photovoltaic panels producing up to 8.75 GWh/year. At first, a significant investment would be needed, but relevant economical savings can follow the installation of photovoltaic panels together with a transition towards heat pumps for space heating and cooling, towards the full electrification of the building sector. Indeed, compared to the district heating scenario – the one among the three others leading to best results – the scenario relying on heat pumps and PV has the potential to further decrease equivalent primary energy consumptions and CO_2 emissions by 43 % and 56 %, respectively.

Considering the simple processing and the ease-to-use of this method, it is possible to foresee an interest among policymakers for the definition of retrofitting campaigns to increase the sustainability of the contemporary city. The target for Turin – together with more than 10000 cities worldwide – is climate neutrality by 2030, as set by the 2019 Covenant of Mayors. The results show that it is still far to be achieved, but significant reductions can be observed compared to the past.

The proposed methodology has shown great potential, and further developments of the research can provide additional knowledge and details to refine the accuracy of the results in absolute terms. One of the strengths of this method is flexibility, with the possibility of adding further information coming from other studies and elaborations to increase the accuracy of the results according to the purpose and the expected output of the study.

Main issues are related to the quality of input data.

Accurate 3D modelling was not the main purpose of this study, but may improve the photovoltaic production estimation by calculating the orientation and inclination of the pitches through programmes – like ENVI LiDAR – which can elaborate 3D point clouds to produce classified vectors of relevant elements, e.g., trees or roofs.

Further, the thermographic pictures were nadiral and influenced by direct solar radiation. Using oblique images, thermal losses through the different parts of the envelope, as well as the share of the vertical walls covered by the windows, would be registered directly, thus enabling a classification which does not require any previous knowledge of the state of the building stock or the calculation through pre-defined parameters. Further simplification of the process can derive from the night acquisition of thermal images. Indeed, the manual classification between sunny and shadowed pitches would be avoided by having homogeneous acquisition conditions, resulting in the – at least partial – automation of the thermal dispersion analysis. Moreover, oblique pictures would allow an easier reconstruction of three-dimensional objects. In this way, the outdoor temperature can be integrated into a 3D model, constituting a first element of a Digital Twin that could be enriched with the addition of further information about the energy performance, like the actual consumption values recorded from the meters to feed physics-based models of each building. However, for the realisation of a Digital Twin the two dimensions of time and space should be properly considered and elaborated according to the purpose for which the digital twin is being created and used, considering the time resolution as strictly dependent on the scale and objective for which the digital twin is used. For the purpose of understanding the energy performance class of buildings, to detect buildings on which renovation is in progress and/or plan for interventions on selected buildings among the building stock, the digital twin should rely on a highly detailed spatial dimension, while the required temporal dimension can be simplified on a yearly based. Therefore, this study represents the first step of a time series to be implemented through yearly data acquisitions to update the model.

Moreover, EPC data are used as both input training and output validation dataset. At this step, a relatively small dataset for training a simple linear regression model was able to provide good results, but an extension of the study area – and thus of the EPC certificates which can be used as input – would make it possible to implement such models. The adoption of an AI-based algorithm, which includes training based on a larger number of EPCs related to a larger city area, is to be explored. In particular, machine learning algorithms would help not only to refine the calculation in the study area, but also to make the extension to other areas easier. By applying these techniques, it would be possible to make the validation parameters more pressing and to perform cross-validation, thus resulting in results with higher quality.

Further extensive studies may be carried out on the retrofitting scenarios, too. Additional studies providing detailed exploration of alternative technologies that are available to meet the targeted improvements of energy class are crucial to explore feasibility issues and quantify the required investments. After having met these two requirements it would be possible to perform financial and economic analyses following the cost-optimal approach suggested at EU level.

Further, the results provided in this study pave the way for a comprehensive study on the potential applicability of Renewable Energy Communities (REC) as recently introduced also in EU legislation, introducing incremental scenarios of sizing and boundaries. This should also be investigated with a view on strategies to ensure energy flexibility and match energy production and consumption. The two scenarios

provided in this study can be used as a reference for setting up a roadmap towards the full implementation of the REC, based on the results provided.

Another crucial issue requiring further development of decarbonization scenarios is the integration in the calculation of the embodied impacts. Considering the latest development and implementation of new technologies, regulations, and practices leading to the recently established high-efficiency standards, it has been demonstrated that embodied energy (and related emissions) has been increasing its weight in buildings' total lifecycle energy use and cannot be neglected when comparing different alternatives for building retrofitting, especially if approached at a district scale (Guidetti & Ferrara, 2023), and therefore should be considered in the policies towards decarbonization of cities.

Declaration of Competing Interest

The authors declare that they have no known competing financial interests or personal relationships that could have appeared to influence the work reported in this paper.

Data availability

Data will be made available on request.

Acknowledgements

This research was developed according to the framework agreement between the City of Turin and the Polytechnic of Turin, signed on 9th February 2023, for the realisation of pilot projects towards the implementation of a Digital Twin. Moreover, our gratitude to DigiSky S.r.l. for providing the thermographic pictures.

References

Bayomi, N., Nagpal, S., Rakha, T., & Fernandez, J. E. (2021). Building envelope modeling calibration using aerial thermography. *Energy and Building, 233*, Article 110648. https://doi.org/10.1016/j.enbuild.2020.110648

Bergamasco, L., & Asinari, P. (2011). Scalable methodology for the photovoltaic solar energy potential assessment based on available roof surface area: Application to Piedmont Region (Italy). *Solar Energy, 85*(5), 1041–1055. https://doi.org/10.1016/j.solener.2011.02.022

Bitelli, G., Conte, P., Csoknyai, T., Franci, F., Girelli, V., & Mandanici, E. (2015). Aerial thermography for energetic modelling of cities. *Remote Sensing (Basel), 7*(2), 2152–2170. https://doi.org/10.3390/rs70202152

'Commission announces 100 cities participating in EU Mission for climate-neutral and smart cities by 2030. (2021) Available at: https://ec.europa.eu/commission/presscorner/detail/en/IP_22_2591'.

Decree 10 November 2011. Regole tecniche per la definizione delle specifiche di contenuto dei database geotopografici. 2011.

'Decreto Legislativo 192/2005'. 2005.

Deng, Z., Chen, Y., Yang, J., & Causone, F. (2023). AutoBPS: A tool for urban building energy modeling to support energy efficiency improvement at city-scale. *Energy and Buildings, 282*. https://doi.org/10.1016/j.enbuild.2023.112794

'Directive 2002/91/EC of the European Parliament and of the Council of 16 December 2002 on the energy performance of buildings'. 2022.

European Commission, (2023). PVGIS (Photovoltaic Geographical Information System) https://re.jrc.ec.europa.eu/pvg_tools/en/.

European Commission, 'A Roadmap for moving to a competitive low carbon economy in 2050. Communication from the Commission to the European Parliament, the European Council, the Council, the European Economic and Social Committee and the Committee of the Regions'. 2011.

European Commission, 'Fit for 55 package'. 2021.

Ferrando, M., Causone, F., Hong, T., & Chen, Y. (2020). Urban building energy modeling (UBEM) tools: A state-of-the-art review of bottom-up physics-based approaches. *Sustainable Cities and Society, 62*, Article 102408. https://doi.org/10.1016/j.scs.2020.102408

Fonseca, J. A., & Schlueter, A. (2015). Integrated model for characterization of spatiotemporal building energy consumption patterns in neighborhoods and city districts. *Applied Energy, 142*, 247–265. https://doi.org/10.1016/j.apenergy.2014.12.068

Gagnon, P., Margolis, R., Melius, J., Phillips, C., & Elmore, R. (2016). Rooftop solar photovoltaic technical potential in the United States. A detailed assessment. *Golden, CO (United States)*. https://doi.org/10.2172/1236153

Green, M. A., Dunlop, E. D., Hohl-Ebinger, J., Yoshita, M., Kopidakis, N., & Hao, X. (2022). Solar cell efficiency tables (version 59). *Progress in Photovoltaics: Research and Applications, 30*(1), 3–12. https://doi.org/10.1002/pip.3506

Guidetti, E., & Ferrara, M. (2023). Embodied energy in existing buildings as a tool for sustainable intervention on urban heritage. *Sustainable Cities and Society, 88*, Article 104284. https://doi.org/10.1016/j.scs.2022.104284

Hofierka, J., & Kaňuk, J. (2009). Assessment of photovoltaic potential in urban areas using open-source solar radiation tools. *Renewable Energy, 34*(10), 2206–2214. https://doi.org/10.1016/j.renene.2009.02.021

International Energy Agency. (2020). *Energy technology perspectives*.

ISTAT, 'Consumi energetici delle famiglie http://dati.istat.it/Index.aspx?DataSetCode=DCCV_CENERG'.

Johari, F., Shadram, F., & Widén, J. (2023). Urban building energy modeling from geo-referenced energy performance certificate data: Development, calibration, and validation. *Sustainable Cities and Society, 96*, Article 104664. https://doi.org/10.1016/j.scs.2023.104664

Koffi, B., Cerutti, A., Duerr, M., Iancu, A., Kona, A., & Janssens-Maenhout, G. (2017). *Covenant of Mayors for Climate and Energy: Default emission factors for local emission inventories*.

Martin, M., Chong, A., Biljecki, F., & Miller, C. (2022). Infrared thermography in the built environment: A multi-scale review. *Renewable and Sustainable Energy Reviews, 165*, Article 112540. https://doi.org/10.1016/j.rser.2022.112540

Ministri dello Sviluppo Economico dell'Ambiente e della Tutela del Territorio e del Mare delle Infrastrutture e dei Trasporti per la Semplificazione della Pubblica Amministrazione. (2015). *Decreto interministeriale 26 Giugno 2015. Adeguamento linee guida nazionali per la certificazione energetica degli edifici*.

Odeh, S., & Nguyen, T. H. (2021). Assessment method to identify the potential of rooftop PV systems in the residential districts. *Energies (Basel), 14*(14), 4240. https://doi.org/10.3390/en14144240

Oraiopoulos, A., & Howard, B. (2022). On the accuracy of urban building energy modelling. *Renewable and Sustainable Energy Reviews, 158*, Article 111976. https://doi.org/10.1016/j.rser.2021.111976

'P9_TA(2023)0068 -TEXTS ADOPTED - Energy performance of buildings (recast) Amendments adopted by the European Parliament on 14 March 2023 on the proposal for a directive of the European Parliament and of the Council on the energy performance of buildings. 2021. [Online]. Available: https://www.europarl.europa.eu/doceo/document/TA-9-2023-0068_EN.pdf.

Pasichnyi, O., Wallin, J., Levihn, F., Shahrokni, H., & Kordas, O. (2019). Energy performance certificates — New opportunities for data-enabled urban energy policy instruments? *Energy Policy, 127*, 486–499. https://doi.org/10.1016/j.enpol.2018.11.051

Pelland, S., & Poissant, Y. (2006). An evaluation of the potential of building integrated photovoltaics in Canada. In *31st annual conference of the solar energy society of Canada (SESCI)*.

R. S. S. p. A. IREN Energia. (2021). *Fattori di conversione in energia primaria e fattori di emissione del vettore energetico teleriscaldamento*.

'SDG11 Lab https://sdg11.polito.it/en/node/37'.

Shang, W.-L., & Lv, Z. (2023). Low carbon technology for carbon neutrality in sustainable cities: A survey. *Sustainable Cities and Society, 92*, Article 104489. https://doi.org/10.1016/j.scs.2023.104489

UNI - Italian Unification Body. (2019). *UNI/TS 11300 (1-2-3-4-5-6) - Prestazioni energetiche degli edifici*.

United Nations, 'Transforming our world: the 2030 Agenda for Sustainable Development'. 2015.

Vecchi, F. (2022). Multi-scalar energy modelling and solar analysis for the urban built environment: The case study of Toronto, Canada. *Politecnico di Torino*.

Wang, C., Ferrando, M., Causone, F., Jin, X., Zhou, X., & Shi, X. (2022). Data acquisition for urban building energy modeling: A review. *Building and Environment, 217*, Article 109056. https://doi.org/10.1016/j.buildenv.2022.109056

Xia, H., Liu, Z., Efremochkina, M., Liu, X., & Lin, C. (2022). Study on city digital twin technologies for sustainable smart city design: A review and bibliometric analysis of geographic information system and building information modeling integration. *Sustainable Cities and Society, 84*, Article 104009. https://doi.org/10.1016/j.scs.2022.104009

Yu, D., & Fang, C. (2023). Urban remote sensing with Spatial Big Data: A review and renewed perspective of urban studies in recent decades. *Remote Sensing (Basel), 15*(5), 1307. https://doi.org/10.3390/rs15051307

Yu, H., et al. (2021). Prioritizing urban planning factors on community energy performance based on GIS-informed building energy modeling. *Energy and Buildings, 249*, Article 111191. https://doi.org/10.1016/j.enbuild.2021.111191

Zheng, H., Gao, G., Zhong, X., & Zhao, L. (2022). Monitoring and diagnostics of buildings' heat loss based on 3D IR model of multiple buildings. *Energy and Buildings, 259*, Article 111889. https://doi.org/10.1016/j.enbuild.2022.111889

Zhou, S., O'Neill, Z., & O'Neill, C. (2018). A review of leakage detection methods for district heating networks. *Applied Thermal Engineering, 137*, 567–574. https://doi.org/10.1016/j.applthermaleng.2018.04.010